



HAL
open science

Comparison between two methodologies for assessing historical earthquake parameters and their impact on seismicity rates In the Western Alps

Ludmila Provost, Andrea Antonucci, Andrea Rovida, Oona Scotti

► To cite this version:

Ludmila Provost, Andrea Antonucci, Andrea Rovida, Oona Scotti. Comparison between two methodologies for assessing historical earthquake parameters and their impact on seismicity rates In the Western Alps. *Pure and Applied Geophysics*, 2022, 179 (2), pp.569-586. 10.1007/s00024-021-02943-4. hal-03658404

HAL Id: hal-03658404

<https://hal.science/hal-03658404>

Submitted on 20 Oct 2022

HAL is a multi-disciplinary open access archive for the deposit and dissemination of scientific research documents, whether they are published or not. The documents may come from teaching and research institutions in France or abroad, or from public or private research centers.

L'archive ouverte pluridisciplinaire **HAL**, est destinée au dépôt et à la diffusion de documents scientifiques de niveau recherche, publiés ou non, émanant des établissements d'enseignement et de recherche français ou étrangers, des laboratoires publics ou privés.

1
2
3
4
5
6
7
8
9
10
11
12
13
14
15
16
17
18
19
20
21
22
23
24
25
26
27
28
29
30
31

COMPARISON BETWEEN TWO METHODOLOGIES FOR ASSESSING HISTORICAL EARTHQUAKE PARAMETERS AND THEIR IMPACT ON SEISMICITY RATES IN THE WESTERN ALPS.

Ludmila Provost, Institut de Radioprotection et Sûreté Nucléaire (IRSN), PSE-ENV, SCAN, BERSSIN, Fontenay-aux-Roses, 92262, France

Andrea Antonucci, Istituto Nazionale di Geofisica e Vulcanologia, Milano, 20133, Italy

Andrea Rovida, Istituto Nazionale di Geofisica e Vulcanologia, Milano, 20133, Italy

Oona Scotti, Institut de Radioprotection et Sûreté Nucléaire (IRSN), PSE-ENV, SCAN, BERSSIN, Fontenay-aux-Roses, 92262, France

Corresponding author: Ludmila Provost, ludmila.provost@irsn.fr

ACKNOWLEDGMENTS

The authors would like to thank Francesco Visini for introducing to the Albarello et al (2001) algorithm used to compute completeness times. Part of the work presented in this paper was done during the lock-down due to the pandemic situation, the authors would like to thank their respective lock-down companions for their patience during our weekly online meetings. The authors would like to thank the two anonymous reviewers for their useful suggestions to improve the article.

ABSTRACT

We investigate the differences in seismicity rate estimates from two historical earthquake catalogues obtained with two methodologies (Boxer and QUake-MD) calibrated on a common dataset of macroseismic intensities and calibration events. The two methodologies were then applied to a test data set of historical earthquakes covering the France, Italy and Switzerland Alpine region. Differences between the resulting magnitude estimates and instrumental magnitudes show a standard deviation of 0.4 for both methodologies, with a mean residual of 0.01 for Boxer and -0.04 for Quake-MD. A systematic difference in magnitude estimates between the two methodologies that correlates with the depth estimated by Quake-MD has been observed. This is attributed to the difference in the treatment of the depth parameter between Boxer and QUake-MD. Nevertheless, differences in magnitude estimates between the two methodologies show a mean residual of 0.006 and a standard deviation of 0.35 resulting in seismicity rates that are not significantly different considering the associated uncertainties. Such results made us believe that the European community could gain in the reduction of epistemic uncertainties associated with the estimate of historical earthquake parameters by agreeing on a common macroseismic and

32 calibration dataset across borders. These efforts should be strongly encouraged. On the other hand, we show that
33 even in the ideal conditions of this benchmark (same calibration events and same macroseismic intensity dataset),
34 methodological differences can lead to systematic differences in magnitude estimates. It is therefore paramount to
35 explore different methodologies for a more realistic quantification of the epistemic uncertainties in estimates of
36 maximum magnitudes and seismic activity rates.

37 KEYWORDS

38 Historical earthquake, parametric earthquake catalogue, seismic activity rate, Western Alps

39 DECLARATIONS

40 This work was funded by IRSN and INGV. The authors do not have any conflict of interest. Data used in this
41 paper are available in the Electronical supplements, and/or from the websites of AHEAD
42 (<https://www.emidius.eu/AHEAD/>) and CPTI15 (<https://emidius.mi.ingv.it/CPTI15-DBMI15/>). The two codes
43 used for deriving earthquake parameters from intensity data are available from: <https://emidius.mi.ingv.it/boxer/>;
44 <https://github.com/ludmilaprvt/QUake-MD>. The third code Matlab_PSHA, used to compute completeness times
45 and annual rates, will be published soon.

46 Figures were made with Matplotlib ([J. D. Hunter, "Matplotlib: A 2D Graphics Environment", Computing in
47 Science & Engineering, vol. 9, no. 3, pp. 90-95, 2007.](#)) and maps with QGIS.

48 INTRODUCTION

49 Researches in many fields, such as seismology, earthquake geology, tectonics, and engineering seismology require
50 the knowledge of the seismicity of the target area to be as long as possible. To this purpose, earthquake parameters
51 determined from intensity data are used to extend the coverage of instrumental earthquake catalogues back to
52 historical times. In Europe, the long history, the type and amount of written documents, and the extensive historical
53 seismological research conducted in the last 50 years translated into one of the world's longest and most detailed
54 record of effects of past earthquakes. This knowledge is represented by several earthquake catalogues (for
55 examples see the AHEAD database; Locati *et al.*, 2014; Rovida and Locati, 2015 and databases at different
56 geographical scales, as well as a wealth of studies on single earthquakes, periods, or areas published over the years.

57 However, the recent analysis in Rovida *et al.* (2020a) highlighted a high fragmentation of repositories of data and
58 a lack of homogeneity in the knowledge of European pre-instrumental seismicity. In particular, the authors show
59 that the geographical distribution of earthquakes with published sets of intensity data is not uniform across Europe,
60 and in some areas, especially in the north and east, historical earthquakes are known only through parametric
61 catalogs, independently of the earthquake size and period of occurrence. Such a fragmentation results from the
62 national perspective adopted in the last decades for the compilation of earthquake databases, with national

63 earthquake catalogues relying on their own input intensity data and their own methodology to determine
64 earthquake locations and magnitudes.

65 A step forward in the harmonization of the knowledge of European past seismicity is represented by the European
66 Archive of Historical Earthquake Data AHEAD (Locati *et al.*, 2014; Rovida and Locati, 2015). It collects the
67 multiplicity of earthquake data of different types and creates relations among them with the aim of making the
68 knowledge of each European earthquake in the period 1000-1899 promptly available. Providing the conclusive
69 macroseismic intensity distribution for every European pre-instrumental earthquake would represent an idealistic
70 ambition, and AHEAD reveals the discrepancies existing in the intensity distributions of earthquakes at country
71 borders, and eases their comparison and the identification of the most representative of the knowledge of each
72 earthquake. Data provided in AHEAD were fully exploited for the compilation of the SHARE European
73 Earthquake Catalogue (SHEEC) 1000-1899 (Stucchi *et al.*, 2013) the input catalogue for the European Seismic
74 Hazard Model ESHM13 (Woessner *et al.*, 2015), and for its update called EPICA – European PreInstrumental
75 earthquake Catalogue (Rovida and Antonucci, 2021).

76 Once a unique base of input data, as harmonized as possible, is built, the compilation of a uniform European
77 earthquake catalogue encounters the problem of assessing robust parameters from it. Several methods for the
78 determination of earthquake parameters from macroseismic information have been proposed since the early ages
79 of modern seismology (see Cecic *et al.*, 1996; and the introduction to Gasperini *et al.*, 2010), from the shape and
80 size of hand-drawn isoseismals, to the analysis and inversion of the spatial distribution of intensity data (e.g. Bakun
81 and Wentworth, 1997; Gasperini *et al.*, 1999; 2010; Musson and Jimenéz, 2008 Provost and Scotti, 2020).
82 However, Bakun *et al.*, (2011) showed some limitations in the most recent and widely used of these methods, each
83 with its own pros and cons, that make the selection of the most reliable solution difficult and not straightforward
84 (Stucchi *et al.*, 2013).

85 In Europe, one of the most evident examples of the variety of data and methods is at the shared borders of
86 Switzerland, France and Italy, where complete and internally consistent macroseismic intensity databases
87 generated the three most advanced historical earthquake catalogues in Europe, respectively ECOS-09 (Fäh *et al.*,
88 2011), F-CAT17 (Manchuel *et al.*, 2018), and CPTI15 (Rovida *et al.*, 2020b). However, being based on different
89 macroseismic databases, and different procedures to assess earthquake parameters they usually provide
90 inconsistent solutions for the very same earthquakes. The consequence of these discrepancies affects all the cross-
91 border elaborations based on these historical catalogues. Among such elaborations, the definition of seismic

92 activity rates, one of the key components of seismic hazard assessment, is particularly influenced by the reliability
93 of the magnitude estimates, as demonstrated in several papers (e.g. Rong *et al.*, 2011; Musson, 2012; Mucciarelli,
94 2014; Beauval *et al.*, 2020). However, none of these works fully explored the effect of the different approaches
95 used for assessing magnitude from macroseismic data.

96 This work aims at first exploring the differences in the macroseismic magnitudes obtained with two alternative
97 methods, Boxer (Gasperini *et al.*, 1999, 2010) and QUake-MD (Provost and Scotti, 2020) to the intensity
98 distributions of pre-instrumental earthquakes at the border between France and Italy (Western Alps region, Figure
99 1). Then, the annual seismic rates calculated from the two different sets of magnitudes are compared in order to
100 quantify the effect of the alternative magnitude determinations.

101

1. SELECTED METHODOLOGIES

102 The methodologies selected in this study are Boxer (Gasperini *et al.*, 1999, 2010) and QUake-MD (Provost and
103 Scotti, 2020). The two methodologies have a downloadable associated software (<https://emidius.mi.ingv.it/boxer/>;
104 <https://github.com/ludmilaprvt/QUake-MD>, respectively) making them good candidates for a comparison study
105 in terms of reproducibility.

106 Boxer incorporates different strategies for jointly determining epicenter location, epicentral intensity I_0 , and
107 magnitude M from intensity data. The “Method 0” (Gasperini *et al.*, 2010) assumes the epicenter as the barycenter
108 of the points with the maximum observed intensities and calculates it as the trimmed (between the 20th and
109 80th percentiles) mean of their coordinates. The epicentral intensity I_0 is assumed equal to the maximum observed
110 value I_{max} , or to $I_{max} - 1$ if less than three I_{max} values are present.

111 The earthquake magnitude is computed as the weighted average of the values independently obtained from each i -
112 th intensity class through the equation by (Sibol *et al.*, 1987):

$$114 \quad M(I) = a(I) + b(I)I_0 + c(I)[\log(\pi D_{epi})]^2 \quad \text{Equation 1}$$

115 where M is magnitude, D_{epi} is the average distance of points with observed intensity I to the calculated epicenter,
116 I_0 is the epicentral intensity, and $a(I)$, $b(I)$, and $c(I)$ are empirical coefficients. The weight is inversely proportional
117 to the number of intensity data and to the square of the standard deviation of the regression for the corresponding
118 intensity class. The explicit computation of depth is excluded from Boxer, and, according to Sibol *et al.* (1987)
119 and Galanopoulos, 1961, the effect of the source depth on the magnitude determination is taken into account by
120 means of the epicentral intensity term in Equation 1.
121

122
123 QUake-MD, acronym for Quantifying Uncertainties for earthquakes' Magnitude and Depth, quantifies
124 uncertainties in magnitude/depth estimates for earthquakes known only by their macroseismic distribution by
125 taking into account the quality of intensity data and the epistemic uncertainties of intensity prediction equations
126 (IPE). Intensity data quality, when available, is used to weight the intensity data points (IDP) in the application of
127 the intensity prediction equations for the magnitude/depth inversion. Intensity data quality is also used to compute
128 uncertainties of the inverted depth and magnitude. IPE epistemic uncertainties are taken into account by the use of
129 different IPEs calibrated for the target region (see Provost and Scotti 2020 for an example). Uncertainties
130 associated to the inverted depth and magnitude combined with the use of different IPEs can be used to build a
131 probability density function of the plausible depth, magnitude and epicentral intensity associated to the considered
132 earthquake. In this exercise, we used the barycenter of the probability density function to compare with other depth
133 and magnitude solutions, i.e. Boxer's outputs or instrumental solutions. QUake-MD IPEs have the following
134 mathematical formulation for describing the attenuation of intensity with epicentral distance:

$$135 \quad I = C_1 + C_2M + \beta \log \left(\sqrt{D_{epi}^2 + H^2} \right) + \gamma \sqrt{D_{epi}^2 + H^2} \quad \text{Equation 2}$$

136 where H is the hypocentral depth, C1 and C2 are the magnitude coefficients, β the geometrical attenuation
137 coefficient and γ the intrinsic attenuation coefficient. In QUake-MD, epicentral location is an input. For the
138 benchmark exercise, Boxer's epicentral locations were taken as input.

139

140 2. CALIBRATION OF METHODOLOGIES ON THE SAME DATASET

141 2.1 DEFINITION OF A COMMON DATASET

142

143 The empirical coefficients of the relations among intensity, magnitude, and depth used in both Boxer and QUake-
144 MD (Equations 1 and 2) need to be calibrated inverting known data of well-assessed recent earthquakes. The
145 reliability of the calibration of both QUake-MD and Boxer depends on the characteristics of the selected calibration
146 dataset. In general, a dataset for calibration purposes must first include earthquakes with reliable instrumental
147 assessments of the magnitude, each with a consistent and plentiful set of intensity data. Such earthquakes must
148 belong to the same tectonic context in order to reflect the same (or similar) propagation and attenuation features
149 of the seismic waves. The dataset should consist of a minimum of 20-30 earthquakes in order to sample the widest
150 possible range of both site intensity values and magnitudes (and epicentral intensities in the case of Boxer). For

151 calibrating the equation used in QUake-MD, a reliable estimate of the focal depth, with associated uncertainty is
152 also necessary.

153
154 The above criteria are not always easily satisfied, especially in areas of low or moderate seismicity (Bakun and
155 Scotti, 2006; Gomez-Capera *et al.*, 2015) such as the Western Alps.

156 To match all the requirements, we built a calibration dataset of 28 earthquakes (Table 1) selected from
157 the macroseismic databases of France (SisFrance/BRGM-EDF-IRSN 2016; Jomard *et al.*, 2021), Switzerland
158 (ECOS-09; Fäh *et al.*, 2011), and Italy (DBMI15; Locati *et al.*, 2019). In case of multiple datasets for the same
159 earthquake, we selected that with highest number of IDPs and with the most complete spatial coverage. To consider
160 as many earthquakes as possible, including large ones, we took into account also earthquakes in the eastern Alps,
161 i.e. outside the study area but within the same seismotectonic context, and those with early although reliable
162 instrumental magnitude measurements from the 1950s and 1960s. Lacking any harmonized instrumental catalogue
163 for the studied border area, magnitudes and depths are selected from different sources available in the literature,
164 as shown in table 1, and include both native moment magnitudes derived from moment tensor solutions, and
165 proxy Mws derived from magnitude estimates in other scales. The magnitude of the selected earthquakes ranges
166 between 3.3 and 6.5 (figure 1, table 1).

167 In the QUake-MD calibration process a-priori depth constraints are explored between a minimum and maximum
168 value given for each event (Hmin and Hmax in table 1) based on either literature or on the statistical analysis in
169 Visini *et al* (2021). A default value of 5 km is associated to events based on LDG estimates. A minimum lower
170 depth limit is fixed at 1 km and a minimum value of 2 km depth uncertainty is assumed. For the application of
171 QUake-MD, depth inversion limits are fixed between 1 and 21 km.

172

#	Date	Area	NObs	Ix	Ref	Lat	Lon	I0	Mw	MwStd	Magnitude reference	Conv.	H	Hmin	Hmax	Depth reference
1	1936-10-18	Alpago Cansiglio	250	9	DBMI15	46,089	12,380	9	5,84	0,14	CPTI15	Yes	13	10	16	(Sandron <i>et al.</i> , 2014)
2	1946-01-25	Ayent	243	8	ECOS-09	46,350	7,400	8	5,80	0,20	(Bernardi <i>et al.</i> , 2005)	Yes	10	1	21	Visini <i>et al.</i> , 2021
3	1946-05-30	Ayent	96	7	ECOS-09	46,300	7,420	7	5,50	0,20	(Bernardi <i>et al.</i> , 2005)	Yes	10	1	21	Visini <i>et al.</i> , 2021
4	1954-05-19	Mayens	80	6	ECOS-09	46,280	7,310	6	5,30	0,43	(Bernardi <i>et al.</i> , 2005)	Yes	10	5	15	ECOS-09
5	1959-04-05	Alpes Provencales	207	7-8	SisFrance	44,533	6,817	7-8	5,52	0,13	CPTI15	Yes	10	1	21	Visini <i>et al.</i> , 2021
6	1960-03-23	Brig	307	7	ECOS-09	46,370	8,020	8	5,00	0,20	(Bernardi <i>et al.</i> , 2005)	Yes	5	1	10	ECOS-09
7	1962-04-25	Vercors	506	7-8	SisFrance	45,033	5,567	7-8	4,98	0,50	(Gomez-Capera <i>et al.</i> , 2015)	Yes	12	7	17	LDG
8	1963-04-25	Vercors	156	7	SisFrance	44,933	5,667	7	4,7	0,19	(Cara <i>et al.</i> , 2015)	No	13	8	18	LDG
9	1964-03-14	Alpnach	362	7	ECOS-09	46,870	8,320	7	5,30	0,30	(Bernardi <i>et al.</i> , 2005)	Yes	5	1	10	ECOS-09
10	1971-09-29	Vorstegstock	295	6	ECOS-09	46,900	9,010	6	4,90	0,15	(Bernardi <i>et al.</i> , 2005)	No	10	1	21	Visini <i>et al.</i> , 2021
11	1976-05-06	Friuli	749	9-10	DBMI15	46,241	13,119	9-10	6,45	0,10	CPTI15	No	5,7	3	8	(Slejko <i>et al.</i> , 1999)
12	1976-12-13	Garda Settentrionale	128	7	ECOS-09	45,894	10,799	7	4,59	0,23	CPTI15	Yes	5,9	1	15	ISC Bulletin
13	1984-04-17	Vercors	90	5-6	SisFrance	44,983	5,167	5-6	4,00	0,19	(Cara <i>et al.</i> , 2015)	No	2	1	7	LDG
14	1988-02-01	Friuli	273	6	DBMI15	46,348	13,076	6	4,82	0,17	CPTI15	Yes	5,1	3	7	OGS Bulletin
15	1989-09-13	Prealpi Vicentine	779	6-7	DBMI15	45,882	11,264	6-7	4,85	0,10	CPTI15	No	9	7	11	OGS Bulletin
16	1990-02-11	Torinese	201	6	DBMI15	44,918	7,558	6	4,56	0,15	CPTI15	Yes	24	20	28	CSII.1
17	1991-11-20	Vaz	374	6	ECOS-09	46,730	9,530	6	4,60	0,30	(Bernardi <i>et al.</i> , 2005)	No	6	3	9	ECOS-09

18	1994-12-14	Genevois	522	6	SisFranc e	45,917	6,367	6	4,28	0,07	(Bernardi <i>et al.</i> , 2005; Braunmiller <i>et al.</i> , 2005)	No	7	4	10	GRN
19	1996-02-27	Dolomiti Friulane	150	5-6	DBMI15	46,309	12,577	5-6	4,31	0,10	CPTI15	Yes	9,5	7	12	OGS Bulletin
20	1996-04-13	Dolomiti Friulane	164	5-6	DBMI15	46,312	12,559	5-6	4,45	0,12	CPTI15	Yes	11,5	9	14	OGS Bulletin
21	1996-07-15	Avant-Pays Savoyard	782	7	SisFranc e	45,917	6,083	7	4,62	0,09	(Braunmiller <i>et al.</i> , 2005)	No	3	1	4	GRN
22	1997-10-31	Prealpes De Digne	90	6	SisFranc e	44,233	6,467	6	4,27	0,18	RCMT	No	6	3	9	GRN
23	1999-01-11	Drac	98	5-6	SisFranc e	45,067	5,733	5-6	3,65	0,19	(Cara <i>et al.</i> , 2015)	No	0	1	3	GRN
24	1999-02-14	Fribourg	123	5	ECOS-09	46,780	7,210	5	3,93	0,22	(Bernardi <i>et al.</i> , 2005; Braunmiller <i>et al.</i> , 2005)	No	2	1	5	ECOS-09
25	1999-09-13	Bas-Plateaux Dauphinois	89	4-5	SisFranc e	45,450	5,417	4-5	3,30	0,15	SED-TDMT	No	4	1	7	GRN
26	2001-07-17	Val Venosta	657	6	DBMI15	46,697	11,074	6	4,78	0,07	CPTI15	No	1	1	12	CSII.1
27	2004-11-24	Garda Occidentale	176	7-8	DBMI15	45,685	10,521	7-8	4,99	0,07	CPTI15	No	5,4	3	8	INGV Bulletin
28	2011-07-25	Torinese	105	5-6	DBMI15	45,016	7,365	5-6	4,67	0,07	CPTI15	No	10	1	21	Visini <i>et al.</i> , 2021

Table 1: List of the earthquake and associated parameters of the calibration dataset. Nobs is the number of intensity data points, Ix is the maximum intensity. The column Ref contains the macroseismic database for the intensity data points. The column Conv. indicates if the magnitude in column Mw is a converted magnitude (Yes) or a native one (No). H is the depth of the earthquakes and Hmin and Hmax are the constraints used in QUake-MD calibration. The column Depth reference gives the reference associated to column H. CPTI15 stands for Catalogo Parametrico dei Terremoti Italiani 2015 (Rovida *et al.*, 2020b), ISC for International Seismological Centre (Storchak *et al.*, 2013), LDG for Laboratoire de Geophysique (Duverger *et al.*, 2021), OGS for Istituto Nazionale di Oceanografia e di Geofisica Sperimentale (<http://www.crs.inogs.it/bollettino/RSFVG/>), GRN for l'Observatoire des Sciences de l'Univers de Grenoble (<https://www.osug.fr/>), CSII.1 for Castello *et al.*, 2006, INGV for Istituto Nazionale di Geofisica e Vulcanologia (<http://terremoti.ingv.it/>)

ECOS-09 for Earthquake Catalogue of Switzerland (Fäh *et al.*, 2011) and DBMI15 for Database Macrosismico Italiano (Locati *et al.*, 2019).

173
174
175

176 In the definition of the calibration dataset we discarded intensities not expressed as numerical values (e.g. “felt”
177 data) and those with intensity lower than 2, while uncertain intensities (e.g. 5-6) are considered
178 as independent classes and assumed as half degrees (e.g. 5.5). Although expressed in different macroseismic
179 scales, for our purposes they can be considered as equivalent, because conversions between scales introduce much
180 higher uncertainties than the differences between the application of the two scales (e.g. Musson *et al.*, 2010; Allen
181 *et al.*, 2012).

182

183 QUake-MD is sensitive to the completeness of the data belonging to each intensity class, which we evaluated
184 comparing the population of each class with the adjacent ones. Using this method, we defined an intensity of
185 completeness for each earthquake (available in Online Resource 1): intensity classes with values smaller than this
186 intensity of completeness are considered as not complete and then not used in QUake-MD calibration. For Boxer
187 we instead used all the data in each class because the number of “complete” IDPs in some intensity classes is not
188 sufficient for calibrating that intensity class, and the calibrations resulting from the complete and the whole
189 datasets are similar. The intensity datasets compiled are made of 8052 data for the whole dataset and 5667 for the
190 “complete” one as shown in figure 2.

191

192 2.2 CALIBRATION PROCESS

193

194 For QUake-MD, we divided the calibration process into two steps, and we assumed γ equal to zero in Equation 2.
195 The first step calibrates the attenuation coefficient β and the second step estimates the magnitude coefficients C1
196 and C2. The attenuation coefficient β is calibrated with the (Kövesligethy, 1907) mathematical formula:

$$197 \quad I = I_0 + \beta \log \left(\sqrt{D_{epi}^2 + H^2} \right) \quad \text{Equation 3.}$$

198 In order to represent the epistemic uncertainty linked to the choice of the dataset, the attenuation is also calibrated
199 with subsets of the calibration dataset as well as with the entire calibration dataset. The subsets were selected
200 according the number of IDP (more than 20 IDP, 100 IDP or 200 IDP), the date of the earthquake (all the
201 earthquakes or only those after 1980), the number of intensity classes (at least 2, 3 or 4 classes), the difference
202 between the epicentral intensity and the intensity of completeness (difference greater than 1, 2 or 3) or the distance
203 of completeness (without this criteria or intensity distributions complete for the first 25 km, i.e. without abrupt
204 changes in data density with distance). Intensity and distance of completeness are defined by expert opinion, based

205 on the change in the slope of the intensity decay with distance and are provided in the Online Resource 1. The
206 calibration with the whole dataset and its subsets results in a distribution of attenuation coefficient values. In the
207 second step, the magnitude coefficients are calibrated with Equation 2. No calibration subsets were built for this
208 step. The magnitude coefficients are calibrated for each attenuation coefficient value obtained in the first step.
209 Three weighting schemes are used in this step: a uniform weighting scheme, a magnitude standard deviation
210 weighting scheme and a magnitude class weighting scheme (see Online Resource 2 for more details about the three
211 weighting schemes). Depth is sequentially inverted in the two steps, within the depth limits defined in Table 1,
212 with the depth value given for each earthquake +/- the associated uncertainties (see Online Resource 2 for more
213 details about depth limits and uncertainties).

214 The Boxer code incorporates a sub-routine to calibrate the coefficients of Equation 1. As described in Appendix 1
215 to Gasperini *et al.*, 2010, the average epicentral distances, trimmed between the 20th and 80th percentiles, of the
216 points in a given intensity class for a given earthquake are calculated first. Classes with less than 4 data and those
217 with intensity greater than the epicentral intensity, calculated by Boxer itself, are excluded from the procedure.
218 The coefficients are then determined by fitting the equation separately for each intensity class and for each
219 earthquake through the minimum weighted sum of the squares. The weights are: i) directly proportional to the
220 number of data points in each intensity class, normalized with the total number of earthquakes in the calibration
221 set that contain intensity of the considered class; and ii) inversely proportional to the square of the standard
222 deviation of the input instrumental magnitude of the corresponding earthquake.

223
224 The described procedure applied to the calibration dataset resulted in the determination of the coefficient for the
225 intensity classes from 2 to 7, including intermediate degrees (e.g. 5-6).

226
227 Both Boxer's and QUake-MD calibrated coefficients are available in the Online Resource3 and Online Resource
228 4 respectively.

229 The reliability of the obtained calibrations of both methods for magnitude estimates is illustrated by the magnitude
230 residual analysis shown in figure 3. The differences between instrumental and macroseismic magnitude
231 are within ± 0.5 Mw units, with an average of 0.03 for Boxer and 0.05 for QUake-MD. Instrumental Mw smaller
232 than 4 tend to be overestimated by Boxer, although there are only 3 earthquakes of this magnitude. Interestingly,
233 these 3 earthquakes (#23, #24 and #25 in Table 1) are all superficial with depth between 0 km and 4 km. Outputs
234 of Boxer and QUake-MD are available in Online Resource 5.

235 As QUake-MD estimates depth along with magnitude, the reliability of QUake-MD calibration is checked for both
236 magnitude and depth in the next section.

237

238

239 2.3 TESTING THE CALIBRATED MODELS

240 2.3.1 TEST DATASET

241 To further test the performance of the obtained calibrations of both QUake-MD and Boxer we applied both
242 methods to an independent test dataset. The dataset was built starting from the same sources of data (i.e. the
243 SisFrance, ECOS-09 and DBMI15 macroseismic databases) and with the same criteria as the calibration dataset,
244 although with a longer time coverage and a majority of converted Mw instead of true ones (Online resource 6). As
245 a whole the test dataset is made of 102 earthquakes in the Alps covering the period 1905 to 2014, with Mw values
246 ranging between 2.7 and 6.1 and 9396 IDPs with maximum intensity from 3 to 9 (figure 4). The test dataset is
247 available in Online resource 6.

248 2.3.2 COMPARISON OF THE MAGNITUDE ESTIMATES FOR THE TEST DATASET

249 We compared first the residual between instrumental magnitude and macroseismic magnitudes (figures 5a and
250 5b). Most magnitude residuals for both methodologies are in the +/- 0.5 range. Standard deviation of the magnitude
251 residuals for both methodologies is equal to 0.4. Boxer's mean magnitude residual is equal to -0.01 and QUake-
252 MD's mean magnitude residual is equal to -0.04. We observe a systematic overestimation of Boxer's and QUake-
253 MD's magnitudes for instrumental magnitudes smaller than 4.0, which exceeds 0.5 for magnitudes smaller than
254 3.5. Magnitudes greater than 5.0 seem underestimated, although the small number of earthquakes with this
255 magnitude and especially greater than 5.5, does not allow us to conclude on a systematic underestimation.

256 Events with residuals exceeding 0.5 are related to four small magnitude events $M_w < 3.3$ for which predictions are
257 extrapolated beyond magnitude used for the calibration or to a specific earthquake for which the instrumental
258 estimate may be overestimated (1920 with magnitude 5.43 Mw). Indeed the instrumental magnitudes reported
259 before the deployment of the World Wide Standardized Seismic Network - WWSSN (i.e., 1960-1964) can be
260 overestimated (Vannucci *et al.*, 2021).

261 Both methodologies present the same bias with magnitude which seems to follow a linear correlation with
262 instrumental magnitudes, i.e. an overestimation of small magnitudes and an underestimation of high magnitudes,

263 with a pivot magnitude equal to 4.5. To confirm this linear correlation we computed the Pearson correlation
264 coefficient for both QUake-MD's and Boxer's magnitude residuals. Pearson correlation coefficient in absolute
265 value can vary from 0 to 1 depending on the strength of the linear relationship between two datasets. An absolute
266 value of the correlation coefficient smaller than 0.5 indicates a weak linear correlation between the two datasets.
267 The Pearson coefficient value for the magnitude of the whole test dataset is equal to 0.6 and 0.8 for QUake-MD
268 and Boxer respectively (violet dashed line in figure 5c and 5d), thus a linear correlation exists between instrumental
269 magnitude and residual magnitude for both methodologies. We then computed the Pearson coefficient for different
270 sliding magnitude window of width equal to 1, from magnitude 2.5 to magnitude 5.5 (see figures 5c and 5d).
271 QUake-MD's residuals present a weak linear correlation with the instrumental magnitude for the windows between
272 3.5 and 5.5, with Pearson coefficient values close to 0.2 for the windows between 4.0 and 5.5 (0.6 for Boxer for
273 the same magnitude window), whereas Boxer's residuals present a weak linear correlation for the 4.5-5.5
274 magnitude window.

275 As a conclusion, both methodologies have the same bias with instrumental magnitude: small magnitudes are
276 overestimated and high magnitudes seem underestimated with a pivot point around Mw 4.5. The linear correlation
277 is weaker around the pivot magnitude equal to 4.5, especially for QUake-MD. The bias does not seem to have a
278 link with the conversion of the instrumental magnitudes to Mw: the residual magnitudes for both methodologies
279 with native Mw follow the same pattern as the converted ones.

280 The comparison of QUake-MD's and Boxer's magnitudes shows (figure 6) that the differences of most magnitudes
281 are smaller than 0.5, with a mean residual between QUake-MD's and Boxer's magnitudes equal to 0.3.
282 Interestingly, there is a systematic difference of magnitude between the two methods due to the inclusion of depth
283 in the QUake-MD inversion scheme which leads to greater magnitudes when the associated depth is deeper than
284 8 km and lower magnitudes when the associated depth is shallower than 8 km.

285 This 8 km value is close to the inverted average depth of 7.77 km computed by Pasolini *et al.* (2008) for Italy
286 based on the same mathematical formulation as Equation 2 used in QUake-MD in this study.

287 2.3.3 COMPARISON OF THE DEPTH ESTIMATES FOR THE TEST DATASET FOR 288 QUAKE-MD

289
290 Figure 7 shows the result of the calibration in terms of depth for QUake-MD for the calibration dataset (figure 7a)
291 and the test dataset (figure 7b). On a total number of 28 earthquakes of the calibration dataset, 19 earthquakes, i.e.

292 67 %, and 66 earthquakes on a total number of 87 earthquakes of the test dataset, i.e 75%, are accurately estimated
293 within an error of +/-5 km. Combined with the good results in magnitude estimates presented in the paper, we
294 consider that the QUake-MD's calibration is satisfactory for the exercise presented in the paper.

295 The largest depth residuals can be explained by a combination of a poorly known instrumental depth (associated
296 uncertainty up to 11 km) and of a poor macroseismic field quality (lack of data). In those cases, it is quite difficult
297 to know what the actual depth of the earthquake is. A detailed analysis of the two calibration earthquakes
298 presenting the largest residual is available in Online Resource 2.

299

300 3. APPLICATION OF THE TWO METHODOLOGIES: IMPACT ON ANNUAL 301 SEISMICITY RATES

302 3.1 PRESENTATION OF THE DATASET WITHIN THE STUDY AREA

303 In this section we explore the impact of the methodological differences in the estimate of macroseismic magnitudes
304 on the estimate of earthquake rates.

305 Focusing on the study area, in the Western Alps (see figure 8), we built two catalogues that share the same
306 instrumental parameters for the period 1981-2015 and same input intensity data for earthquakes in the period 1000-
307 1980, but are processed with Boxer and QUake-MD separately. The earthquakes within the study area are mapped
308 in the figure 8. The catalogues with the earthquakes in the period 1000-1980 processed with Boxer and QUake-
309 MD are called hereafter Boxer's catalogue and QUake-MD's catalogue, respectively.

310 Macroseismic data were selected among those provided in AHEAD for the period 1000-1899, and for the period
311 1900-1980 in its Italian counterpart - the Italian Archive of Historical Earthquake Data ASMI
312 (<https://doi.org/10.13127/asmi>; Rovida *et al.*, 2017), that covers the study area. For each earthquake we selected
313 the dataset with the largest number of data and derived from the most complete historical investigation (see Online
314 Resource 7). For the instrumental part we used the instrumental catalogue at the basis of CPTI15, which consists
315 of instrumental locations from Italian instrumental catalogues selected according to a temporal priority scheme
316 and Mw following the procedures in Lolli *et al.*, 2020.

317 The selected events consist of 232 earthquakes, 189 of which are in the period 1000-1980. The magnitude of the
318 latter was determined with both QUake-MD and Boxer and we kept in the catalogue 65 events after applying the
319 following criteria to ensure the reliability of the results: Boxer magnitudes calculated with all IDPs (not from
320 epicentral intensity) and only earthquakes with more than 3 IDP. Following these criteria, the older event in the

321 output catalogues occurred in 1564. The catalogue, with both Boxer and QUake-MD estimates, is available in
322 Online Resource 7.

323 3.2 MAGNITUDE COMPARISON

324 Boxer's and QUake-MD's magnitude estimates are in good agreement (see figure 9), with a mean residual equal
325 to 0.006 and a standard deviation equal to 0.35. Except for three events, differences between the two methodologies
326 in magnitude estimates are less than 0.5 units. The same difference between the two methods due to the inclusion
327 of depth in QUake-MD inversion scheme as in figure 6 is observed: QUake-MD magnitudes greater than Boxer's
328 are associated to depth estimates greater than 8 km, and smaller QUake-MD magnitudes are associated to depth
329 shallower than 8 km. Thus, depending on whether the region of study is dominated by shallow or deep events, the
330 use of one method or another may lead to important differences in the estimate of the observed maximum
331 magnitude.

332 3.3 ANNUAL SEISMIC ACTIVITY RATES COMPARISON

333 In order to compute comparable annual seismic activity rates from the Boxer's and QUake-MD catalogues, we
334 applied the same declustering and completeness estimate methods to both catalogues. The space-time windowing
335 declustering technique of Knopoff and Gardner, 1972 and Gardner and Knopoff, 1974, with window's length
336 modified according to Burkhard and Grünthal (2009) as implemented in the last version of the ZMap software
337 (Wiemer, 2001), identifies the same clusters for both catalogues. However, the main event of each cluster was not
338 necessarily the same for both catalogues. Nevertheless, the magnitudes associated to the main events for both
339 catalogue in this study area were close with a mean difference of 0.1. These differences did not affect the following
340 steps of earthquake rates estimates, because the main events of each cluster were classified in the same magnitude
341 class.

342 In order to apply the same methodology to both catalogues, we used the algorithm of Albarello *et al.*, 2001. The
343 method tests differences in occurrence rates of events in different time intervals, using a binomially distributed
344 random variable. The completeness probability is then calculated using a conditional probability. We chose a
345 minimum magnitude of completeness at Mw 3.5 and considered a magnitude bin width of 0.5.

346 Mean and quantiles of the obtained distribution of completeness times for each catalogue (figure 10) differ mainly
347 for magnitudes greater than 4.5 due to the reduced number of earthquakes in this magnitude range and their
348 difference in higher magnitude estimates.

349 Finally, we estimated earthquake rates applying the same completeness times to both catalogues corresponding to
350 the most recent completeness time of both distributions for each bin. In this way, each catalog should be
351 theoretically complete. We used a minimum magnitude of 3.5 and a magnitude bin width of 0.25.

352 The incremental annual rates for Boxer's and QUake-MD's catalogues are presented figure 11a. Not surprisingly,
353 the annual rates of the two first magnitude bins are identical: according to the completeness time (equal to 1976)
354 only instrumental earthquakes are in these bins. The two following magnitude bins, in which both instrumental
355 and historical earthquakes are present, similar annual rates are estimated for both catalogues. The annual rates for
356 magnitudes higher than 4.5 are quite different.

357 The small number of earthquakes in the highest bin leads to annual seismic activity rates more sensitive to
358 magnitude differences between the two catalogues due to the different treatment of depth in the two methodologies.
359 However, given the small number of events in these bins, the observed differences in annual seismic activity rates
360 should not be considered statistically significant as shown by the error bars computed with the Weichert method
361 shown in Figure 11a.

362

363 DISCUSSIONS AND CONCLUSIONS

364 The purpose of this paper is to perform a benchmarking exercise to quantify the differences in the estimates of
365 historical earthquake magnitudes determined with different methodologies, namely Boxer and the QUake-MD,
366 calibrated with the same sets of macroseismic and instrumental data. We then compare the annual seismic activity
367 rates resulting from the two parametric earthquake catalogues obtained from the two methodologies applied to the
368 same intensity distributions of historical earthquakes.

369 One of the main differences between the two methodologies is the treatment of the hypocentral depth of the
370 earthquakes, and the determination of the epicentral location. In Boxer, the depth is implicitly taken into
371 account through the epicentral intensity value in the estimate of magnitude from the macroseismic field.
372 Magnitude estimates are then less influenced by eventually biased depth estimates. However, in case of sources
373 with depth significantly different from the mean of the calibration dataset, the use of the epicentral intensity as
374 proxy for depth may affect the accuracy of the magnitude estimate. Estimating depth is paramount especially for
375 events which have depth that maybe significantly different from the mean depth of the study area. In QUake-MD
376 both depth and magnitude are deduced from the macroseismic field. However, estimates of depth can be biased

377 by poor quality macroseismic fields. Since magnitude and depth values are correlated, magnitude can be also
378 biased. In those cases, fixing depth or reducing the acceptable depth limits in QUake-MD is strongly encouraged
379 (Provost and Scotti, 2020). In this case, if magnitude estimates are on average less influenced by potentially biased
380 depth estimates, the magnitude of events much deeper than the average depth of the calibration events are most
381 likely underestimated.

382 We show that the two methodologies offer equivalent results in terms of magnitude estimates when calibrated with
383 the same dataset, although they are quite different in their approach to estimate magnitude. Systematic
384 differences between the two methods (higher magnitudes for QUake-MD estimates compared to Boxer's for events
385 deeper than 8 km) are shown to be due to difference in the way depth is considered. As a consequence, according
386 to the results presented here, earthquake rates based on the catalogues compiled with the two methodologies are
387 similar, as long as earthquakes in any given magnitude bin present a range of depths balanced around 8 km, as for
388 example for $M < 4.5$. On the other hand, for areas with either prevailing very shallow or deep seismic activity, a
389 bias could exist between the magnitude estimates of the two methodologies, and thus on the corresponding annual
390 seismic activity rates. Finally, although differences in annual seismic activity rates observed in the study area
391 between the two methodologies for $M > 4.5$ are statistically poorly constrained, conclusions may differ in regions
392 with higher seismic activity, in particular when considering only magnitudes $M_w > 4.5$ to compute frequency-
393 magnitude distributions.

394 Estimate of the parameters of historical earthquakes are associated with large uncertainties depending on the
395 method chosen to estimate those parameters, the calibration database for the chosen method or the completeness
396 of the intensity distributions, that sum to the uncertainties deriving from the assessment of macroseismic intensity
397 from documental information. Such uncertainties should be thoroughly considered throughout a seismic hazard
398 assessment, whereas they are usually disregarded. We believe that sharing the same data for the calibration
399 earthquakes, i.e. instrumental magnitude, depth, and location and macroseismic data among neighboring countries,
400 as well as the same macroseismic data for the historical earthquakes, would help reducing the differences between
401 magnitude estimates across borders. However, building on the experience of this study and depending on the
402 purpose of a seismic hazard assessment study, it may be worth exploring different methodologies to
403 convert macroseismic data into earthquake parameters to ensure that the range of plausible earthquake rates are
404 sampled. Indeed, the uncertainties in earthquake parameters derived from one methodology only could be
405 insufficient to represent the actual epistemic uncertainty of such estimates.

406

407 **FIGURES CAPTIONS**

408 **Fig. 1 : Epicentral location, magnitude, and number of intensity data points (IDP) of each earthquake in**
409 **the calibration dataset. Numbers indicate the earthquakes as in Table 1. Each earthquake is represented**
410 **by a circle. The circle size represents the magnitude of the earthquake: the bigger the magnitude**
411 **earthquake, the bigger the size. Color of the circle represent the number of IDP (column NObs in table 1)**
412 **associated to each earthquake: the darker the color, the smaller the number of IDP.**

413 **Fig. 2 : Calibration dataset: frequencies of the intensity values for the whole (light gray on the figure) and**
414 **the complete (dark gray on the figure) dataset (NN = non-numerical values). Complete dataset means all**
415 **data within complete intensity classes, i.e. intensities greater than their associated intensity of**
416 **completeness. The whole dataset includes all available IDPs, excluding intensity levels smaller than 2.**

417 **Fig. 3 : Residuals between instrumental and macroseismic magnitude estimates for QUake-MD (a) and**
418 **Boxer (b) as a function of instrumental magnitude for the calibration earthquakes used in this study. The**
419 **horizontal dashed lines represent the +/- 0.5 values of magnitude residuals. A dark blue color (black points**
420 **in non-color version) is used to identify earthquakes with native Mw and a yellow color (light gray in non-**
421 **color version) is used to identify earthquakes with Mw magnitudes coming from conversion of another**
422 **type of magnitude.**

423

424 **Fig. 4 : Test dataset: epicentral location, magnitude, and number of intensity data (IDP) for each**
425 **earthquake in the test dataset. Each earthquake is represented by a circle. The circle size represents the**
426 **magnitude of the earthquake: the bigger the magnitude earthquake, the bigger the size. Color of the circle**
427 **represent the number of IDP (column NObs in Table 1) associated to each earthquake: the darker the**
428 **color, the smaller the number of IDP.**

429 **Fig. 5 : Comparison between instrumental and macroseismic magnitude residual for QUake-MD (c) and**
430 **Boxer (d) as a function of instrumental magnitude for the test data set. A dark blue color (black points in**
431 **non-color version) is used to identify earthquakes with native Mw and a yellow color (light gray in non-**
432 **color version) is used to identify earthquakes with Mw magnitudes coming from conversion of another**
433 **type of magnitude. Top figures: Pearson coefficient for the entire dataset (dashed violet lines) and for**
434 **sliding magnitude windows of one unit width (gray lines) for QUake-MD (a) and Boxer (b). The subplots**
435 **(a) and (b) a horizontal dotted line is added at Pearson coefficient value of 0.5.**

436 **Fig. 6 : Comparison of QUake-MD and Boxer magnitudes for the 102 earthquakes of the test dataset. A**
437 **1:1 black line is added, as well as dashed lines representing the +/- 0.5 magnitude difference around the**
438 **1:1 line. The colors represent the values of QUake-MD depth. White color is associated to depth equal to 8**
439 **km. Earthquakes with depths deeper than 8 km are mostly above the 1:1 line and earthquakes with**
440 **depths shallower than 8 km are mostly under the 1:1 line.**

441 **Fig. 7: Residual depth as a function of magnitude and depth residuals for the calibration dataset (left**
442 **figure) and the test dataset (right figure). Residuals are computed by subtracting instrumental values and**
443 **QUake-MD's values. In both figures, the solid black lines represent the 0 residual, the horizontal dashed**
444 **lines represent the +/- 5 km depth residual and the vertical dashed lines represent the +/- 0.5 unit**
445 **magnitude residual.**

446

447 **Fig. 8 : Earthquakes in the study area (black polygon). Blue (the darker gray in non-color version) points**
448 **represent the post-1980 earthquakes and the red (the lighter gray in non-color version) points represent**

449 the historical earthquakes, i.e. earthquakes that occurred before 1980, including 1980. The insert map
450 shows the location of the study area at a larger scale.

451 **Fig. 9 :** Comparison of Boxer and QUake-MD magnitudes for the study area A 1:1 black line is added, as
452 well as dashed lines representing the +/- 0.5 magnitude difference around the 1:1 line. The colors
453 represent the values of QUake-MD depth. White color is associated to depth equal to 8 km. Earthquakes
454 with depths deeper than 8 km are mostly above the 1:1 line and earthquakes with depths shallower than 8
455 km are mostly under the 1:1 line.

456 **Fig. 10 :** Completeness time distribution obtained by the application of the Albarello 2001 algorithm for
457 the Boxer and QUake-MD catalogues, with the magnitude-time distribution for the Boxer's catalogue (a)
458 and QUake-MD's catalogue (b). Filled lines represent the mean of the completeness time distribution and
459 the dashed lines the quartiles. A blue (darker gray in non-color version) color is used for Boxer and red
460 (lighter gray) color is used for QUake-MD.

461 **Fig. 7 :**(a) Incremental annual rates for Boxer and QUake-MD catalogues. Vertical lines represent the
462 annual seismicity rates uncertainty computed as described in Weichert (1980). A blue (darker gray in
463 non-color version) color and a square symbol are used for Boxer and red (lighter gray) color and a circle
464 symbol are used for QUake-MD. The QUake-MD symbols are slightly shifted to the right for better
465 readability of the figure. (b) Number of earthquakes per magnitude bin used to compute the annual
466 seismicity rates for the Boxer's catalogue (blue bars) and QUake-MD's catalogue (red bars).

ONLINE RESOURCE CAPTIONS

468 **ESM_1.xlsx :** Additional information to the calibration list presented in table 1 of the main text

469 **ESM_2.pdf :** additional information about QUake-MD calibration procedure and macroseismic fields of two
470 calibration earthquake.

471 **ESM_3.xlsx :** output file of Boxer calibration with Boxer's model coefficients

472 **ESM_4.xlsx :** QUake-MD's coefficients after calibration

473 **ESM_5.xlsx :** Results of the application of Boxer and QUake-MD on the calibration dataset

474 **ESM_6.xlsx :** List of the test dataset

475 **ESM_7.xlsx :** Boxer's and QUake-MD catalogues for the study area

REFERENCES

477

478 Albarello, D., R. Camassi, and A. Rebez (2001). Detection of space and time heterogeneity in the completeness
479 of a seismic catalog by a statistical approach: An Application to the Italian Area, *Bull. Seismol. Soc. Am.*
480 **91**, no. 6, 1694–1703, doi: 10.1785/0120000058.

481 Allen, T. I., D. J. Wald, and C. B. Worden (2012). Intensity attenuation for active crustal regions, *J. Seismol.* **16**,
482 no. 3, 409–433, doi: 10.1007/s10950-012-9278-7.

483 Bakun, W. H., A. G. Capera, and M. Stucchi (2011). Epistemic Uncertainty in the Location and Magnitude of
484 Earthquakes in Italy from Macroseismic Data, *Bull. Seismol. Soc. Am.* **101**, no. 6, 2712–2725, doi:
485 10.1785/0120110118.

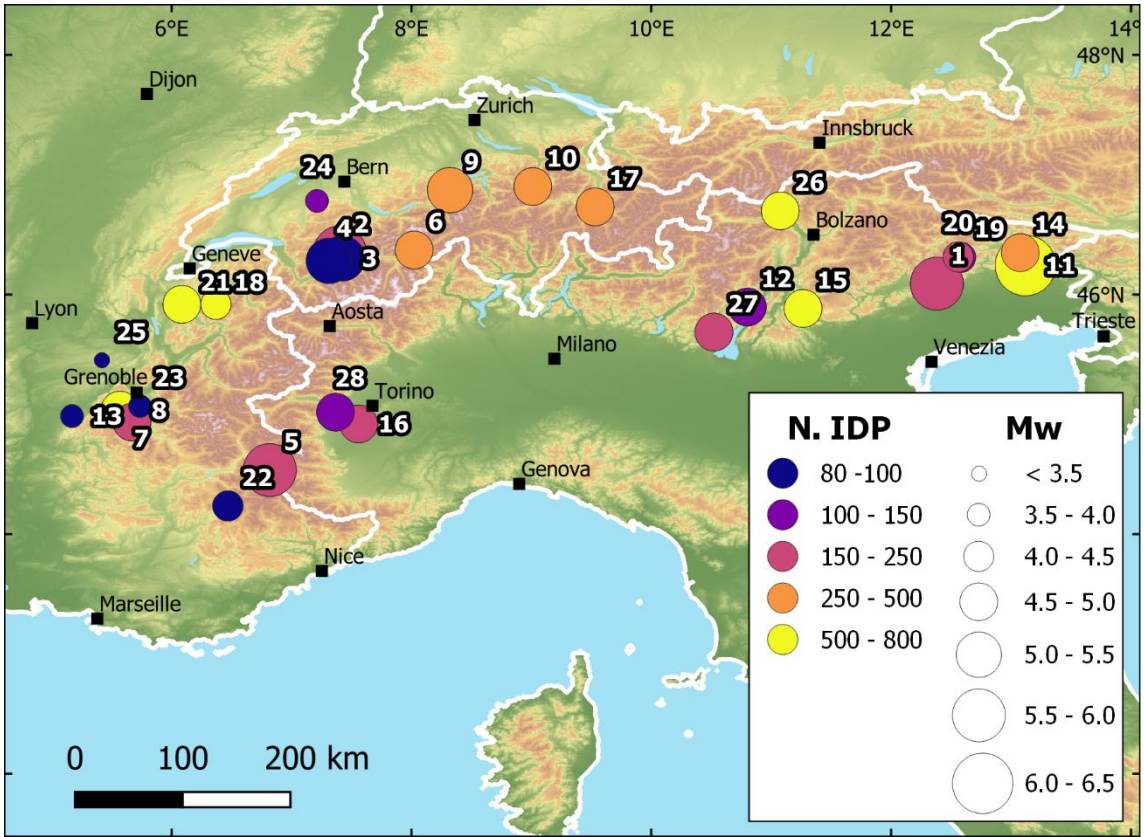
- 486 Bakun, W. H., and O. Scotti (2006). Regional intensity attenuation models for France and the estimation of
487 magnitude and location of historical earthquakes, *Geophys. J. Int.* **164**, no. 3, 596–610, doi:
488 10.1111/j.1365-246X.2005.02808.x.
- 489 Bakun, W. H., and C. M. Wentworth (1997). Estimating Earthquake Location and Magnitude from Seismic
490 Intensity Data, *Bull. Seismol. Soc. Am.* **87**, no. 6, 1502–1521.
- 491 Beauval, C., P.-Y. Bard, and L. Danciu (2020). The influence of source- and ground-motion model choices on
492 probabilistic seismic hazard levels at 6 sites in France, *Bull. Earthq. Eng.* **18**, no. 10, 4551–4580, doi:
493 10.1007/s10518-020-00879-z.
- 494 Bernardi, F., J. Braunmiller, and D. Giardini (2005). Seismic Moment from Regional Surface-Wave Amplitudes:
495 Applications to Digital and Analog Seismograms, *Bull. Seismol. Soc. Am.* **95**, no. 2, 408–418, doi:
496 10.1785/0120040048.
- 497 Braunmiller, J., sed M. W. Group, N. Deichmann, sed M. W. Group, D. Giardini, sed M. W. Group, S. Wiemer,
498 and sed M. W. Group (2005). Homogeneous Moment-Magnitude Calibration in Switzerland, *Bull.*
499 *Seismol. Soc. Am.* **95**, no. 1, 58–74, doi: 10.1785/0120030245.
- 500 Burkhard, M., and G. Grünthal (2009). Seismic source zone characterization for the seismic hazard assessment
501 project PEGASOS by the Expert Group 2 (EG1b), 1, *Swiss J. Geosci.* **102**, no. 1, 149–188, doi:
502 10.1007/s00015-009-1307-3.
- 503 Cara, M., Y. Cansi, A. Schlupp, P. Arroucau, N. Béthoux, E. Beucler, S. Bruno, M. Calvet, S. Chevrot, A. Deboissy,
504 et al. (2015). SI-Hex: a new catalogue of instrumental seismicity for metropolitan France, *Bull. Soc.*
505 *Geol. Fr.* **186**, no. 1, 3–19, doi: 10.2113/gssgfbull.186.1.3.
- 506 Castello, B., G. Selvaggi, C. Chiarabba, and A. Amato (2006). CSI Catalogo della sismicità italiana 1981-2002,
507 versione 1.1, *Ist. Naz. Geofis. E Vulcanol. INGV*, doi: 10.13127/CSI.1.1.
- 508 Cecic, I., R. M. W. Musson, and M. Stucchi (1996). Do seismologists agree upon epicentre determination from
509 macroseismic data? A survey of ESC Working Group ' Macroseismology', 5, *Ann. Geophys.* **39**, no. 5,
510 doi: 10.4401/ag-4031.
- 511 Duverger, C., G. Mazet-Roux, L. Bollinger, A. G. Trilla, A. Vallage, B. Hernandez, and Y. Cansi (2021). A decade of
512 seismicity in metropolitan France (2010–2019): the CEA/LDG methodologies and observationsUne
513 décennie de sismicité en France métropolitaine (2010–2019) : les méthodes et observations du
514 CEA/LDG, *Bull. Société Géologique Fr.* **192**, no. 1, doi: 10.1051/bsgf/2021014.
- 515 Fäh, D., D. Giardini, P. Kästli, N. Deichmann, M. Gisler, G. Schwarz-Zanetti, S. Alvarez-Rubio, S. Sellami, B.
516 Edwards, B. Allmann, et al. (2011). ECOS-09, Earthquake Catalogue of Switzerland - Release 2011,
517 SED/ECOS/R/001/20110417, Swiss Seismological Service, ETH Zürich.
- 518 Galanopulos, A. G. (1961). On magnitude determination by using macroseismic data, *Ann. Geophys.* **14**, 225–
519 253.
- 520 Gardner, J. K., and L. Knopoff (1974). Is the sequence of earthquakes in Southern California, with aftershocks
521 removed, Poissonian?, *Bull. Seismol. Soc. Am.* **64**, no. 5, 1363–1367.
- 522 Gasperini, P., F. Bernardini, G. Valensise, and E. Boschi (1999). Defining seismogenic sources from historical
523 earthquake felt reports, *Bull. Seismol. Soc. Am.* **89**, no. 1, 94–110.
- 524 Gasperini, P., G. Vannucci, D. Tripone, and E. Boschi (2010). The Location and Sizing of Historical Earthquakes
525 Using the Attenuation of Macroseismic Intensity with Distance, *Bull. Seismol. Soc. Am.* **100**, no. 5A,
526 2035–2066, doi: 10.1785/0120090330.

- 527 Gomez-Capera, A. A., A. Rovida, P. Gasperini, M. Stucchi, and D. Viganò (2015). The determination of
528 earthquake location and magnitude from macroseismic data in Europe, *Bull. Earthq. Eng.* **13**, no. 5,
529 1249–1280, doi: 10.1007/s10518-014-9672-3.
- 530 Jomard, H., O. Scotti, S. Auclair, P. Dominique, K. Manchuel, and D. Sicilia (2021). The SISFRANCE database of
531 historical seismicity. State of the art and perspectives, *Comptes Rendus Géoscience* **353**, no. S1, 1–24,
532 doi: 10.5802/crgeos.91.
- 533 Knopoff, L., and J. K. Gardner (1972). Higher Seismic Activity During Local Night on the Raw Worldwide
534 Earthquake Catalogue, *Geophys. J. Int.* **28**, no. 3, 311–313, doi: 10.1111/j.1365-246X.1972.tb06133.x.
- 535 Kövesligethy, R. (1907). Seismischer Stärkegrad und Intensität der Beben, *Gerlands Beitr. Zur Geophys.* **8**, 21–
536 103.
- 537 Locati, M., R. D. Camassi, A. N. Rovida, E. Ercolani, F. M. A. Bernardini, V. Castelli, C. H. Caracciolo, A. Tertulliani,
538 A. Rossi, R. Azzaro, *et al.* (2019). Italian Macroseismic Database DBMI15, version 2.0, report, doi:
539 <https://doi.org/10.13127/DBMI/DBMI15.2>.
- 540 Lolli, B., G. Paolo, E. Biondini, and G. Vannucci (2020). The relationship between ML and Mw for small
541 earthquakes (ML < 2-4) in Italy, **22**, 18821.
- 542 Meletti, C., W. Marzocchi, V. D’Amico, G. Lanzano, L. Luzi, F. Martinelli, B. Pace, A. Rovida, M. Taroni, and F.
543 Visini (2021). The new Italian seismic hazard model (MPS19), *Ann. Geophys.* **64**, no. 1, doi:
544 <https://doi.org/10.4401/ag-8579>.
- 545 Mucciarelli, M. (2014). Uncertainty in PSHA related to the parametrization of historical intensity data, *Nat.*
546 *Hazards Earth Syst. Sci.* **14**, no. 10, 2761–2765, doi: <https://doi.org/10.5194/nhess-14-2761-2014>.
- 547 Musson, R. (2012). The Effect of Magnitude Uncertainty on Earthquake Activity Rates, *Bull. Seismol. Soc. Am.*
548 **102**, 2771–2775, doi: 10.1785/0120110224.
- 549 Musson, R. M. W., G. Grünthal, and M. Stucchi (2010). The comparison of macroseismic intensity scales, *J.*
550 *Seismol.* **14**, no. 2, 413–428, doi: 10.1007/s10950-009-9172-0.
- 551 Musson, R. M. W., and M. J. Jimenez (2008). Macroseismic estimation of earthquake parameters, NA4
552 deliverable, NEREIS Project.
- 553 Pasolini, C., D. Albarello, P. Gasperini, V. D’Amico, and B. Lolli (2008). The Attenuation of Seismic Intensity in
554 Italy, Part II: Modeling and Validation, *Bull. Seismol. Soc. Am.* **98**, no. 2, 692–708, doi:
555 10.1785/0120070021.
- 556 Provost, L., and O. Scotti (2020). QUake-MD: Open-Source Code to Quantify Uncertainties in Magnitude–Depth
557 Estimates of Earthquakes from Macroseismic Intensities, *Seismol. Res. Lett.* **91**, no. 5, 2520–2530, doi:
558 10.1785/0220200064.
- 559 Rong, Y., M. Mahdyar, B. Shen-Tu, and K. Shabestari (2011). Magnitude problems in historical earthquake
560 catalogues and their impact on seismic hazard assessment, *Geophys. J. Int.* **187**, no. 3, 1687–1698, doi:
561 10.1111/j.1365-246X.2011.05226.x.
- 562 Rovida, A., and M. Locati (2015). Archive of Historical Earthquake Data for the European-Mediterranean Area,
563 in *Perspectives on European Earthquake Engineering and Seismology: Volume 2* A. Ansal(Editor),
564 Springer International Publishing, Cham, Geotechnical, Geological and Earthquake Engineering, 359–
565 369, doi: 10.1007/978-3-319-16964-4_14.
- 566 Rovida, A., M. Locati, R. Camassi, A. Antonucci, F. M. A. Bernardini, C. H. Caracciolo, and L. Maffezzoni (2017).
567 L’Archivio Storico Macrosismico Italiano (ASMI).

- 568 Rovida, A., M. Locati, R. Camassi, B. Lolli, and P. Gasperini (2020). The Italian earthquake catalogue CPTI15, *Bull.*
569 *Earthq. Eng.* **18**, no. 7, 2953–2984, doi: 10.1007/s10518-020-00818-y.
- 570 Sandron, D., G. Renner, A. Rebez, and D. Slejko (2014). Early instrumental seismicity recorded in the eastern
571 Alps, *Boll. Geofis. Teor. Ed Appl.* **55**, no. 4, 755–788, doi: 10.4430/bgta0118.
- 572 Scotti, O., D. Baumont, G. Quenet, and A. Levret (2004). The French macroseismic database SISFRANCE:
573 objectives, results and perspectives, *Ann. Geophys.* **47**, no. 2/3, 11.
- 574 Sibol, M. S., G. A. Bollinger, and J. B. Birch (1987). Estimation of magnitudes in central and eastern North
575 America using intensity and felt area, *Bull. Seismol. Soc. Am.* **77**, no. 5, 1635–1654.
- 576 Slejko, D., R. Camassi, I. Cecic, D. Herak, M. Herak, S. Kociu, V. Kouskouna, J. Lapajne, K. Makropoulos, C.
577 Meletti, *et al.* (1999). Seismic hazard assessment for Adria, *Ann. Geofis.* **42**, no. 6.
- 578 Storchak, D. A., D. D. Giacomo, I. Bondár, E. R. Engdahl, J. Harris, W. H. K. Lee, A. Villaseñor, and P. Bormann
579 (2013). Public Release of the ISC–GEM Global Instrumental Earthquake Catalogue (1900–2009),
580 *Seismol. Res. Lett.* **84**, no. 5, 810–815, doi: 10.1785/0220130034.
- 581 Vannucci, G., B. Lolli, and P. Gasperini (2021). Inhomogeneity of Macroseismic Intensities in Italy and
582 Consequences for Macroseismic Magnitude Estimation, *Seismol. Res. Lett.* **92**, no. 4, 2234–2244, doi:
583 10.1785/0220200273.
- 584 Visini, F., B. Pace, C. Meletti, W. Marzocchi, A. Akinci, R. Azzaro, S. Barani, G. Barberi, G. Barreca, R. Basili, *et al.*
585 (2021). Earthquake Rupture Forecasts for the MPS19 Seismic Hazard Model of Italy, 2, *Ann. Geophys.*
586 **64**, no. 2, SE220–SE220, doi: 10.4401/ag-8608.
- 587 Weichert, D. (1980). Estimation of the earthquake recurrence parameters for unequal observation periods for
588 different magnitudes, *Bull. Seismol. Soc. Am.* **70**, no. 4, 1337–1346.
- 589 Wiemer, S. (2001). A Software Package to Analyze Seismicity: ZMAP | Seismological Research Letters |
590 GeoScienceWorld, *Seismol. Res. Lett.* **72**, no. 3, 373–382, doi: <https://doi.org/10.1785/gssrl.72.3.373>.

591

592 **FIGURES**



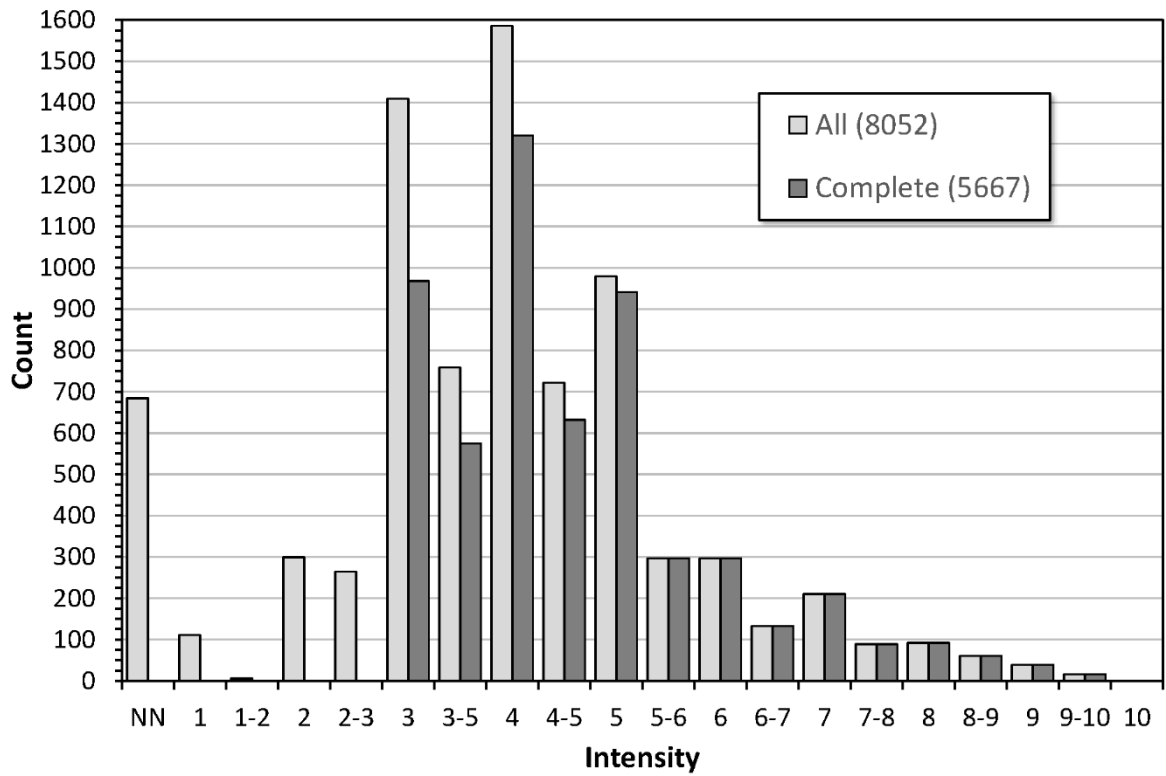
593

594 **Fig. 1**

595

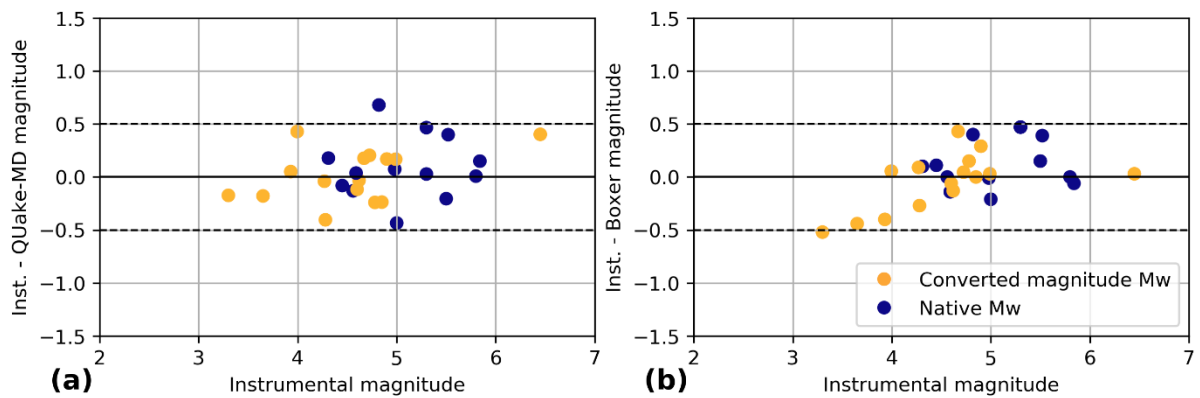
596

597



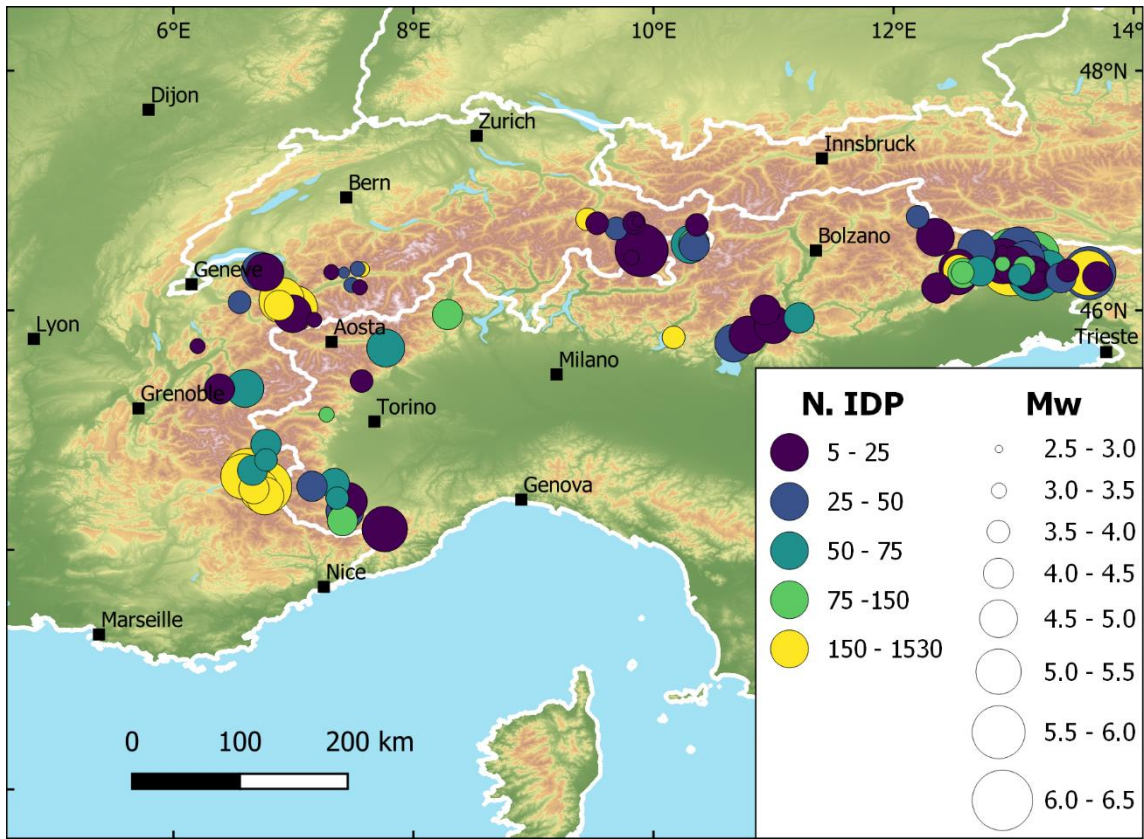
598

599 **Fig. 2**



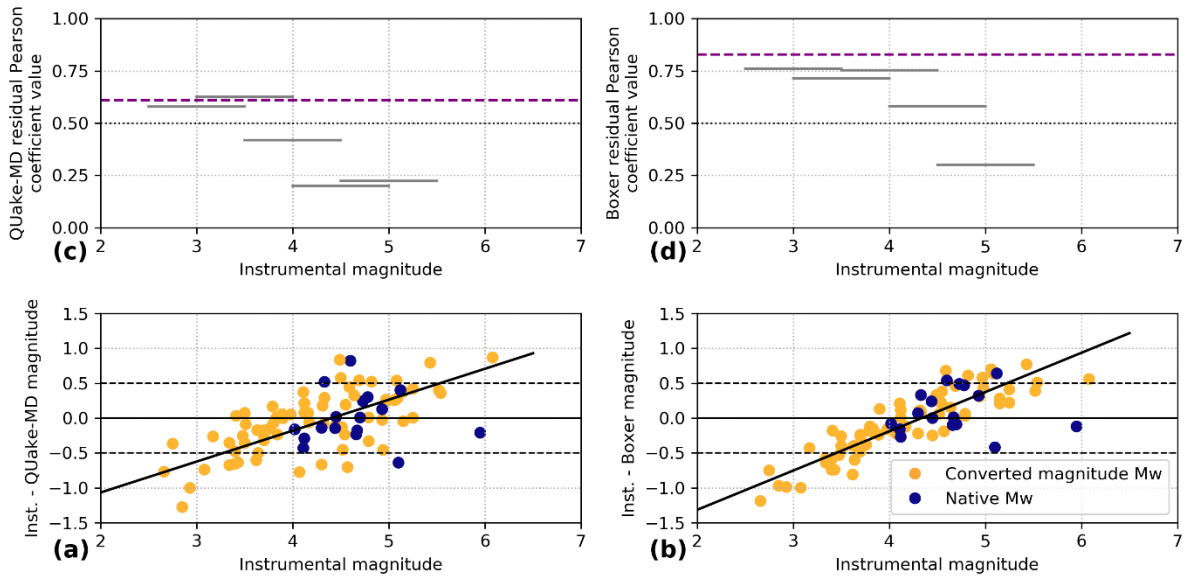
600

601 **Fig. 3**



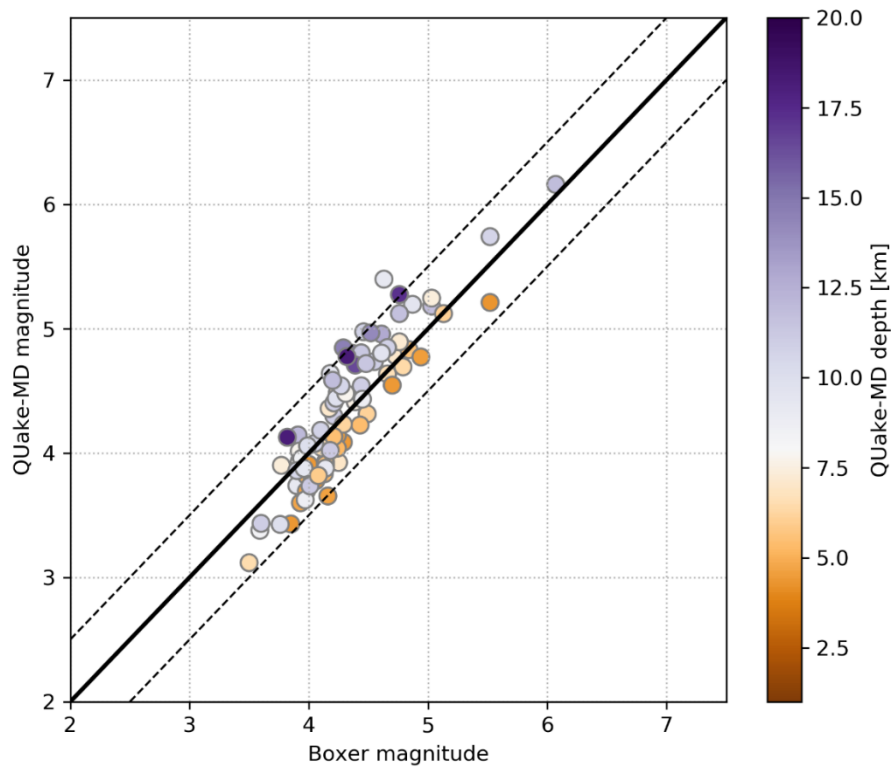
602

603 **Fig. 4**



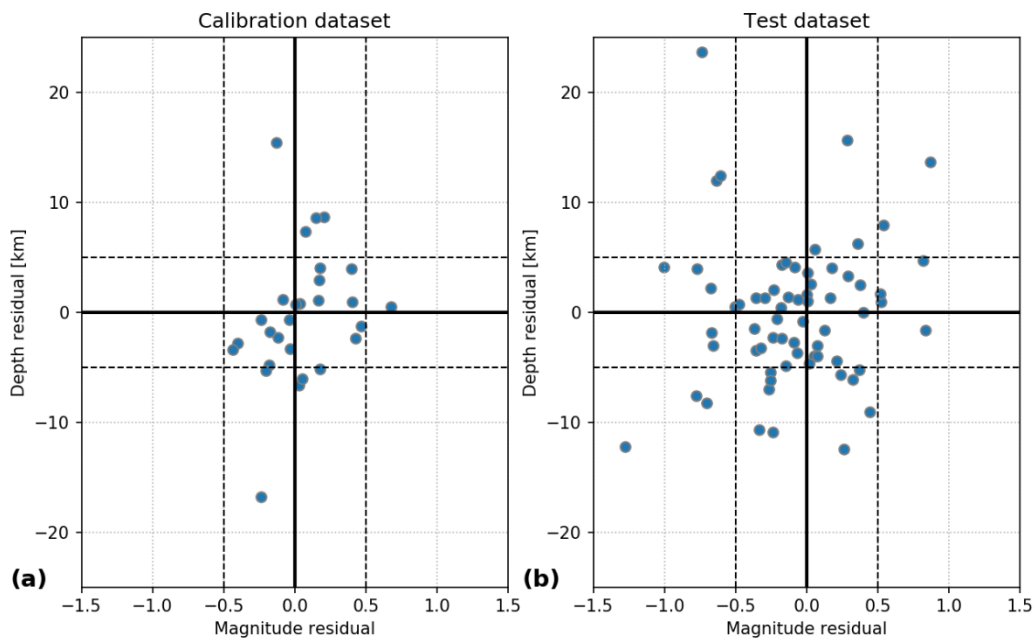
604

605 **Fig. 5**



606

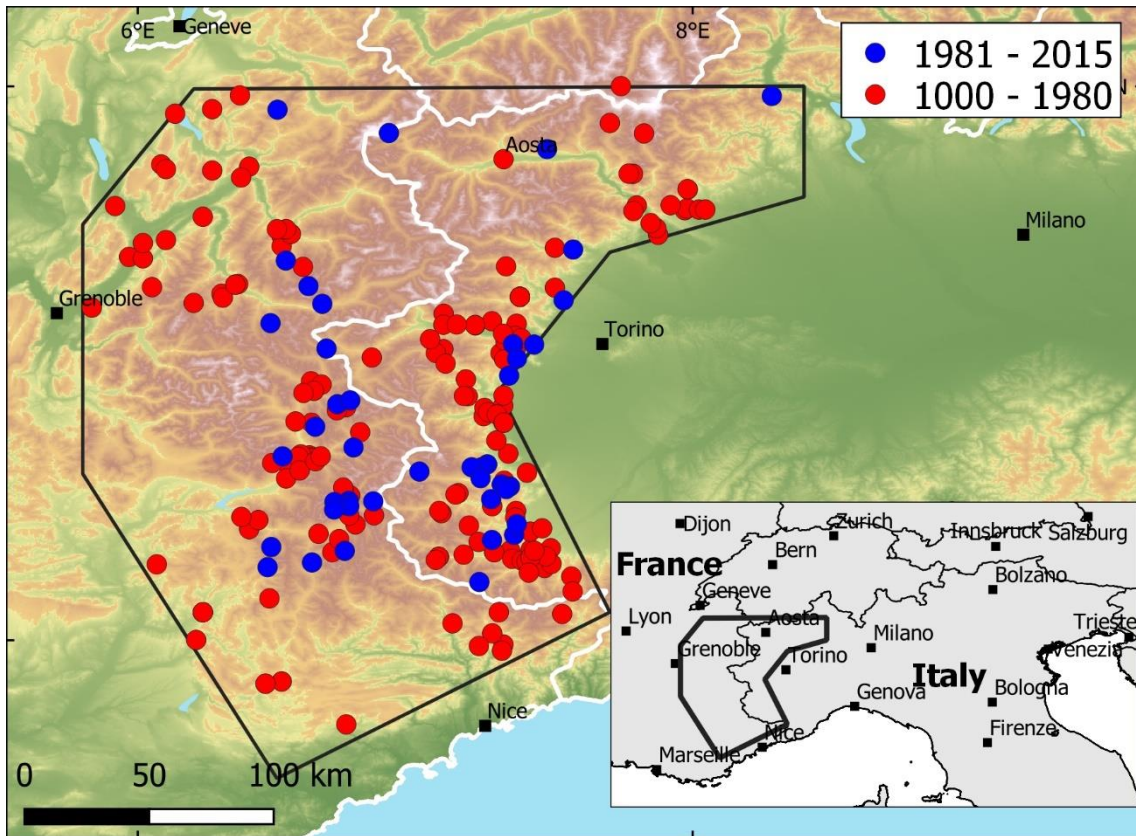
607 **Fig. 6**



608

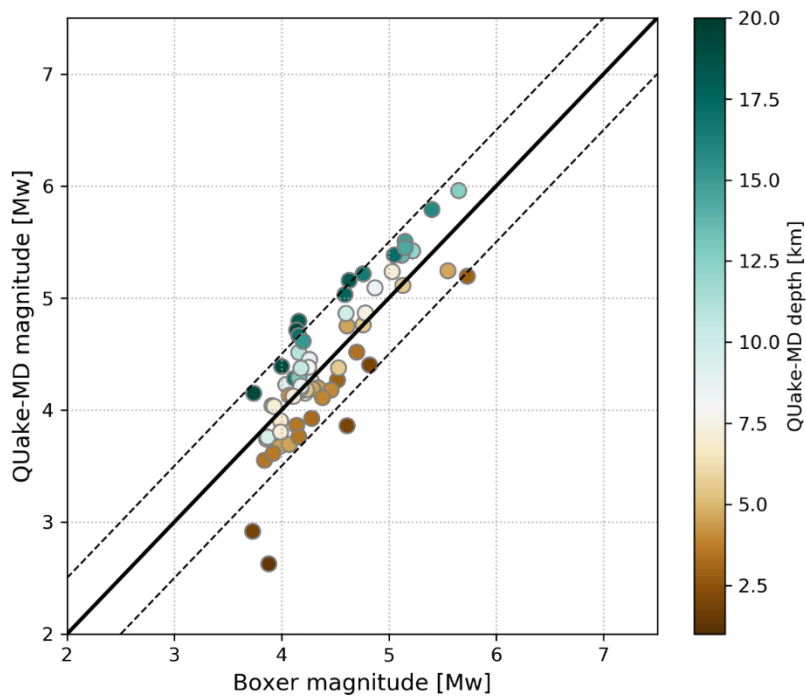
609 **Fig. 7**

610



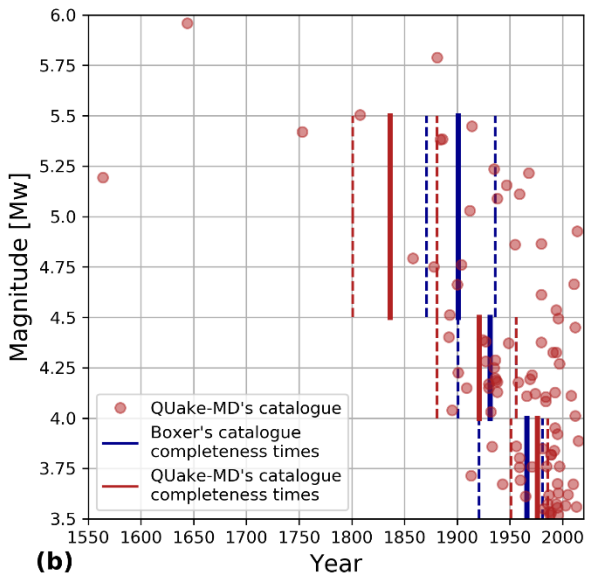
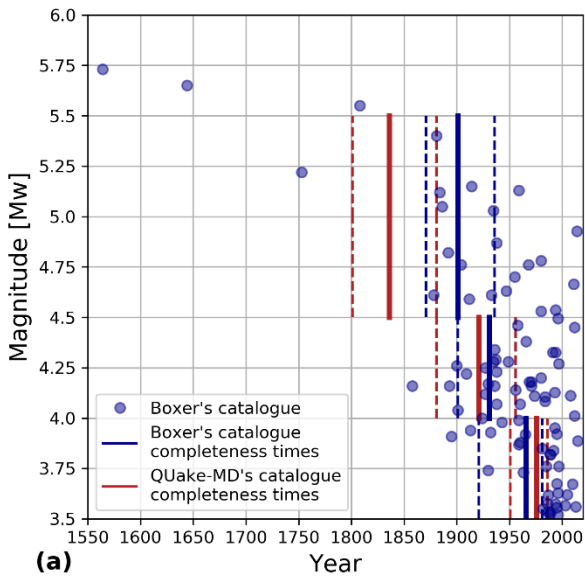
611

612 **Fig. 8**



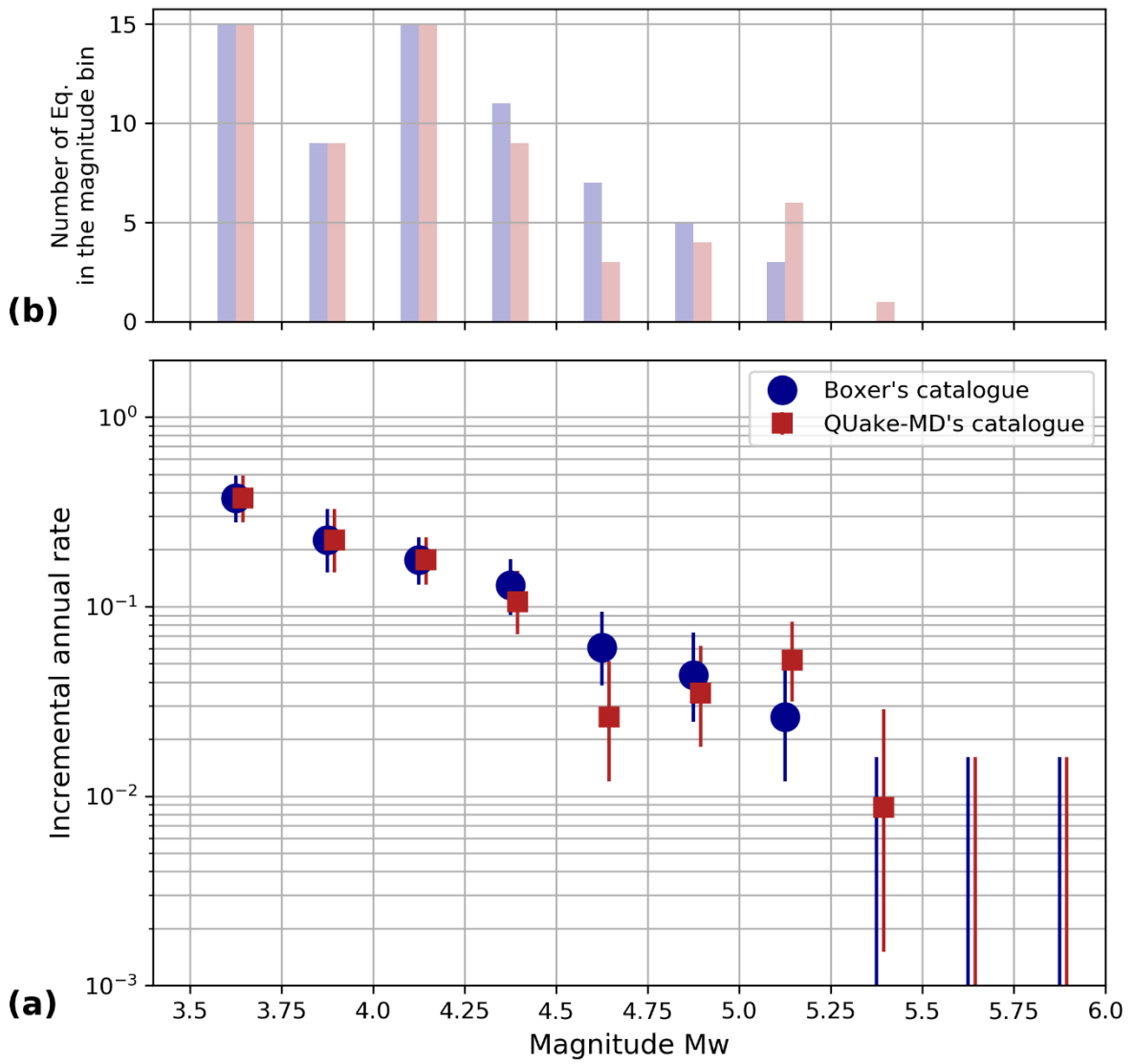
613

614 **Fig. 9**



615

616 Fig. 10



617

618 Fig. 11